J. Fluid Mech. (1977), *vol.* 80, *part* 4, *pp.* 609–615
Printed in Great Britain

Second-order spectral local isotropy in turbulent scalar fields

BY C. W. VAN ATTA
Scripps Institution of Oceanography,
University of California, La Jolla

(Received 20 August 1976 and in revised form 25 November 1976)

This work was motivated by recent experimental results on the spectra of fluctuating temperature gradients in a heated turbulent boundary layer obtained by Sreenivasan, Danh & Antonia. Standard techniques of turbulence theory are used herein to derive expressions relating the individual one-dimensional spectra of each of the three components of the spatial gradient $\partial\theta/\partial x_i$ in a locally isotropic turbulent scalar field. The results of the isotropic theory explain all of the new observed features of the temperature-gradient spectra. The spectra of $\partial\theta/\partial y$ and $\partial\theta/\partial z$ decrease monotonically with increasing wavenumber, in contrast to the well-known behaviour of the spectrum of $\partial\theta/\partial x$, which reaches a maximum value at roughly one-tenth the Kolmogorov wavenumber. The spectra of $\partial\theta/\partial y$ and $\partial\theta/\partial z$ are relatively rich in low frequency energy and relatively poor in high frequency energy compared with the spectrum of $\partial\theta/\partial x$. The absolute magnitudes of the spectra of $\partial\theta/\partial y$ and $\partial\theta/\partial z$ calculated from the spectrum of $\partial\theta/\partial x$ using the isotropic relations are in generally good agreement with the corresponding measured spectra for a large range of wavenumbers, indicating second-order spectral local isotropy of the fine-scale scalar structure for sufficiently large wavenumbers. The form of the spectra of $\partial\theta/\partial y$ and $\partial\theta/\partial z$ in the inertial subrange is derived analytically.

1. Introduction

The Kolmogorov (1941*a*, *b*) hypothesis of local isotropy that spectral properties of turbulence should obey isotropic relations for sufficiently large wavenumbers is one of the cornerstones of turbulence theory. For the fluctuating velocity field, local tests of isotropy are usually applied to second-order spectral quantities, e.g. through the isotropic relation between spectra of longitudinal and lateral components of velocity fluctuations. Some tests have also been based on third-order spectral quantities, e.g. those used by Van Atta & Chen (1969) and by Helland (1974). Second-order spectral tests for local isotropy of turbulent scalar fields have not been considered in previous work, apparently because of a lack of appropriate measurements that would have stimulated formulation of the simple theory required. An appropriate stimulus is the recent data of Sreenivasan, Danh & Antonia (1976), which produced several interesting new results whose interpretation was not clear in the absence of any theoretical guidance. The present paper describes an attempt to understand these results.

Sreenivasan *et al.* (1976) made simultaneous measurements of all three spatial derivatives of the fluctuating temperature θ in a heated turbulent boundary layer.

Their spectral measurements show that the spectrum of $\partial\theta/\partial x$ contains significantly more high frequency energy and less low frequency energy than the spectra of $\partial\theta/\partial y$ and $\partial\theta/\partial z$. Believing this behaviour to be at variance with expectations based on local isotropy, they suggested that it was probably a result of the moderate Reynolds number of their flow. In the present work theoretical relations between the spectra of $\partial\theta/\partial x$, $\partial\theta/\partial y$ and $\partial\theta/\partial z$ are derived for isotropic turbulence and their consequences are compared with the measurements. The predicted form of the one-dimensional spectra of $\partial\theta/\partial y$ and $\partial\theta/\partial z$ is found to be distinctly different from that of $\partial\theta/\partial x$ for all Reynolds numbers. The theoretical results correctly predict the shape and magnitude of the spectra of $\partial\theta/\partial y$ and $\partial\theta/\partial z$, and explain the observed amplitudes relative to the spectrum of $\partial\theta/\partial x$ at low and high frequencies. The results quantitatively show that for sufficiently large wavenumbers the temperature field is in fact nearly locally isotropic with respect to second-order spectral quantities.

2. Theory

Let the three-dimensional scalar field be represented by a Fourier–Stieltjes integral (e.g. Batchelor 1953, pp. 31 and 184)

$$\theta(\mathbf{x}) = \iiint e^{i\mathbf{k}\cdot\mathbf{x}}\, dZ_\theta(\mathbf{k}) \tag{1}$$

so that

$$\frac{\partial\theta(\mathbf{x})}{\partial x_i} = i\iiint k_i\, e^{i\mathbf{k}\cdot\mathbf{x}}\, dZ_\theta(\mathbf{k}), \quad i = 1, 2, 3. \tag{2}$$

Then the correlation function of $\partial\theta/\partial x_i$ is

$$\left\langle \frac{\partial\theta(\mathbf{x}+\mathbf{r})}{\partial x_i}\frac{\partial\theta(\mathbf{x})}{\partial x_i}\right\rangle = \iiint k_i^2\, e^{i\mathbf{k}\cdot\mathbf{r}}\, \Phi(\mathbf{k})\, d\mathbf{k}, \quad i = 1, 2, 3, \tag{3}$$

where $\Phi(\mathbf{k}) = \Phi(k)$ is the spectral density field in three dimensions of the isotropic scalar field θ, and repeated indices are not summed. Taking $\mathbf{r}$ along the mean flow direction x_1, we have

$$\left\langle \frac{\partial\theta(x+r)}{\partial x_i}\frac{\partial\theta(x)}{\partial x_i}\right\rangle = \int_0^\infty \exp(ik_1 r)\left[2\iint_{-\infty}^{\infty} k_i^2\, \Phi(k)\, dk_2\, dk_3\right] dk_1, \quad i = 1, 2, 3. \tag{4}$$

The expression in square brackets gives the (measurable) one-dimensional spectrum of $\partial\theta/\partial x_i$, i.e.

$$\phi_{\theta_x}(k_1) = \iint_{-\infty}^{\infty} 2k_1^2\, \Phi(k)\, dk_2\, dk_3 \tag{5}$$

and similarly for $\partial\theta/\partial y$ and $\partial\theta/\partial z$. For isotropy

$$\phi_{\theta_y}(k_1) = \phi_{\theta_z}(k_1) = \iint (k_2^2 + k_3^2)\, \Phi(k)\, dk_2\, dk_3 = \iint (k^2 - k_1^2)\, \Phi(k)\, dk_2\, dk_3. \tag{6}$$

Defining the usual three-dimensional spectrum averaged over spherical shells

$$F(k) = 4\pi k^2 \Phi$$

and performing the integrations over k_2 and k_3 with k_1 fixed, $k^2 = k_1^2 + k_2^2 + k_3^2 = k_1^2 + \sigma^2$ and $\sigma\, d\sigma = k\, dk$, we have

$$\phi_{\theta_y}(k_1) = \phi_{\theta_z}(k_1) = \tfrac{1}{2}\left[\int_{k=k_1}^{\infty} kF(k)\, dk - k_1^2 \int_{k=k_1}^{\infty} k^{-1}F(k)\, dk\right]. \tag{7}$$

Similarly, from (5) we recover the familiar relation

$$\phi_{\theta_x}(k_1) = k_1^2 \phi_\theta(k_1) = k_1^2 \int_{k_1}^{\infty} k^{-1} F(k)\, dk, \tag{8}$$

where

$$F(k) = -k\partial\phi_\theta/\partial k \tag{9}$$

as given, for example, in Hinze (1975, p. 285).

In terms of the one-dimensional spectra (7) becomes

$$\phi_{\theta_y}(k_1) = \phi_{\theta_z}(k_1) = \int_{k_1}^{\infty} k\phi_\theta(k)\, dk = \int_{k_1}^{\infty} k^{-1}\phi_{\theta_x}(k)\, dk, \tag{10}$$

or

$$\phi_{\theta_x}(k_1) = -k_1\,\partial\phi_{\theta_y}/\partial k_1. \tag{11}$$

Since $\phi_{\theta_y}(k_1)$ is the integral of $k\phi_\theta(k)$ from k_1 to ∞, it must be a monotonically decreasing function of k_1, in sharp contrast to the spectrum of ϕ_{θ_x}, which increases with k_1 for small k_1 (like $k_1^{\frac{1}{3}}$ in the inertial–convective subrange) and then decreases for large k_1. Since $\phi_{\theta_x}(k) < \phi_{\theta_y}(k) = \phi_{\theta_z}(k)$ for small k and

$$\int_0^{\infty} \phi_{\theta_x}(k)\, dk = \int_0^{\infty} \phi_{\theta_y}(k)\, dk,$$

ϕ_{θ_x} and ϕ_{θ_y} must cross over at some value of k, and we must have $\phi_{\theta_y}(k) < \phi_{\theta_x}(k)$ for large k. In § 3 we shall see that this relative behaviour is observed in the experiments.

This behaviour is qualitatively similar to the relation between the one-dimensional spectra of the transverse and longitudinal velocity components, $\phi_v(k_1) = \phi_w(k_1)$ and $\phi_u(k_1)$ respectively, in incompressible locally isotropic turbulence. For this case (see, for example, Batchelor 1953, p. 50)

$$\phi_v(k_1) = \tfrac{1}{2}\phi_u(k_1) - \tfrac{1}{2}k_1\, d\phi_u(k_1)/dk_1. \tag{12}$$

The corresponding differences between the spectral transformations from one to three dimensions for the velocity vector $\mathbf{u}$ and scalar-gradient vector $\nabla\theta \equiv \partial\theta/\partial\mathbf{x}$ are due to the fact that

$$\nabla . \mathbf{u} = 0 \tag{13}$$

whereas

$$\nabla \times \nabla\theta = 0. \tag{14}$$

The spectral equivalents of (13) and (14) imply, respectively, that

$$k_i\, dZ_i(\mathbf{k}) = 0, \quad k_i k_i\, dZ_\theta(\mathbf{k}) = k^2 dZ_\theta(\mathbf{k}), \qquad (15),(16)$$

i.e. the Fourier coefficient vector of the incompressible velocity field is perpendicular to the wavenumber vector (Batchelor 1953, p. 32), whereas the Fourier coefficient vector of the scalar-gradient field is parallel to the wavenumber vector. It is interesting to note that for a random isotropic sound field, for which $\nabla \times \mathbf{u} = 0$ but $\nabla . \mathbf{u} \neq 0$, we have (e.g. Panchev 1971, p. 117)

$$\phi_v(k_1) = \int_{k_1}^{\infty} k^{-1}\phi_u(k)\, dk$$

and the spectral relations are formally the same as those for the components of $\nabla\theta$.

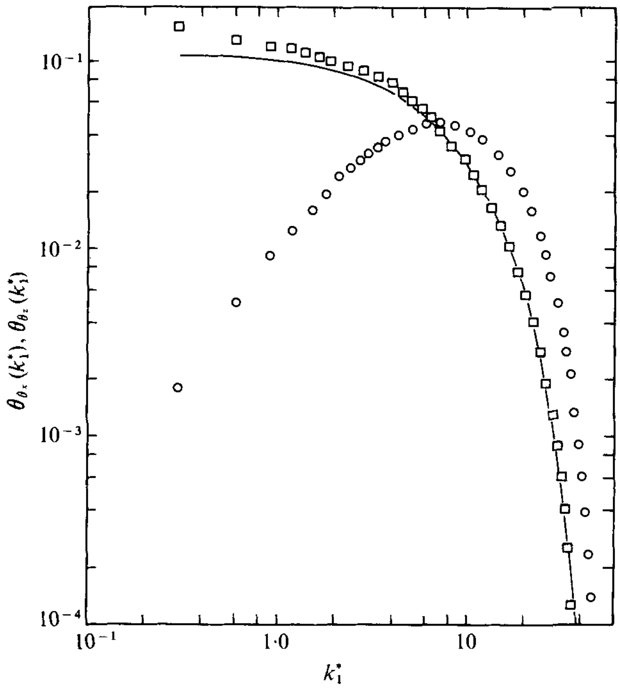

FIGURE 1. Normalized spectra of $\partial\theta/\partial z$ and $\partial\theta/\partial x$. Four-wire probe data of Sreenivasan *et al.*: □, $\phi_{\theta_z}(k_1^*)$; ○, $\phi_{\theta_x}(k_1^*)$; ——, $\phi_{\theta_z}(k_1^*)$ computed from measured $\phi_{\theta_x}(k_1^*)$ using the isotropic relation (10).

The form of ϕ_{θ_y} and ϕ_{θ_z} in the inertial–convective subrange can be derived from (11). In the inertial–convective subrange

$$\phi_{\theta_x}(k_1) = \beta\langle\epsilon\rangle^{-\frac{1}{3}}\langle\chi\rangle k_1^{\frac{1}{3}}, \tag{17}$$

where $\langle\epsilon\rangle$ and $\langle\chi\rangle$ are the mean rates of dissipation of kinetic energy and scalar variance, respectively, and β is a constant. So from (11) we have

$$\partial\phi_{\theta_y}(k_1)/\partial k_1 = -\beta\langle\epsilon\rangle^{-\frac{1}{3}}\langle\chi\rangle k_1^{-\frac{2}{3}}. \tag{18}$$

Integrating once we find

$$\phi_{\theta_y}(k_1) = \phi_{\theta_z}(k_1) = \phi_{\theta_y}(\hat{k}_1) - 3\beta\langle\epsilon\rangle^{-\frac{1}{3}}\langle\chi\rangle(k_1^{\frac{1}{3}} - \hat{k}_1^{\frac{1}{3}}), \tag{19}$$

where $\hat{k}_1$ is the low wavenumber limit of the inertial–convective subrange.

Equation (19) implies that to examine experimental data for ϕ_{θ_y} and ϕ_{θ_z} for power-law behaviour it would be most useful to work with the quantity

$$\phi_{\theta_y}(\hat{k}_1) + 3\beta\langle\epsilon\rangle^{-\frac{1}{3}}\langle\chi\rangle\hat{k}_1^{\frac{1}{3}} - \phi_{\theta_y}(k_1),$$

as a log–log plot of this quantity versus k_1 would then have a slope of $+\frac{1}{3}$ in the inertial–convective subrange.

3. Comparison with experiments

Sreenivasan *et al.* (1976) made simultaneous measurements of all three components of the fluctuating temperature gradient in the inner region of a fully developed

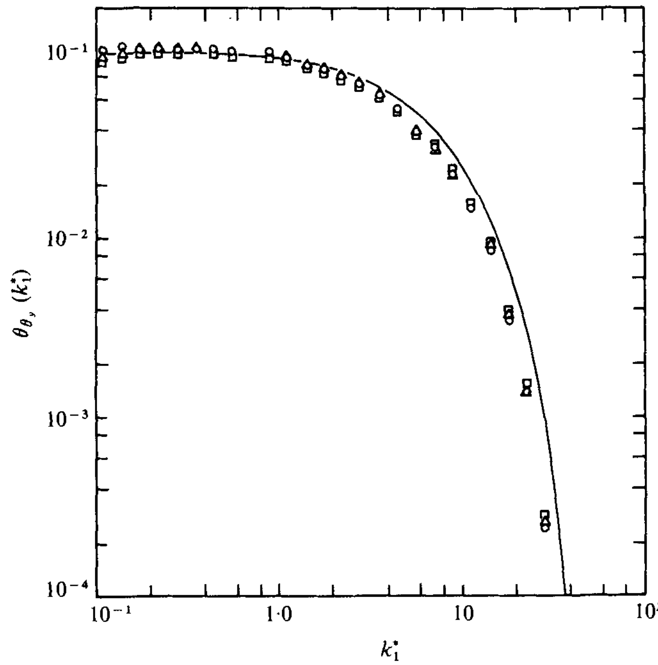

FIGURE 2. Normalized spectrum of $\partial\theta/\partial y$. Two-wire probe data of Sreenivasan *et al.* for $\phi_{\theta_y}(k_1^*)$: ○, $\Delta y = 5{\cdot}25\eta_\theta$; △, $\Delta y = 4{\cdot}1\eta_\theta$; □, $\Delta y = 3\eta_\theta$. Here η_θ is the Corrsin–Oboukhov scale, equal to $1{\cdot}28\eta$, where $\eta = \nu^{\frac{3}{4}}/\langle\epsilon\rangle^{\frac{1}{4}}$ is the Kolmogorov scale. ——, $\phi_{\theta_y}(k_1^*)$ computed from measured $\phi_{\theta_z}(k_1^*)$ using the isotropic relation (10).

turbulent boundary layer over a heated flat plate at a moderate Reynolds number. In their notation, the x co-ordinate designates the streamwise direction, the y co-ordinate is normal to the plate and the z co-ordinate designates the spanwise direction. Their cold-wire measurements were made with a four-wire probe consisting of two parallel vertical wires measuring $\partial\theta/\partial z \cong \Delta\theta/\Delta z$ mounted a small distance upstream of two parallel horizontal wires measuring $\partial\theta/\partial y \cong \Delta\theta/\Delta y$. The streamwise derivative $\partial\theta/\partial x$ was obtained from the time derivative of θ using Taylor's frozen-turbulence hypothesis. The separation of the vertical wires measuring $\partial\theta/\partial z$ was 1·2 mm, while the separation of the horizontal wires measuring $\partial\theta/\partial y$ was 0·9 mm. Measurements with a two-wire probe with various separations were also made.

The experimental data for ϕ_{θ_x}, ϕ_{θ_y} and ϕ_{θ_z}, obtained at a height above the plate equal to 0·126 times the velocity boundary-layer thickness with a free-stream velocity U of about 9 m/s, are shown in figures 1 and 2. For these data, the turbulence Reynolds number $R_\lambda = u'\lambda/\nu \approx 150$, where u' is the r.m.s. longitudinal velocity fluctuation, λ the Taylor microscale and ν the kinematic viscosity. There is no evidence of an inertial–convective subrange in ϕ_{θ_x}, as expected for such a small R_λ, and useful comparison with (19) cannot be made because both β and $\hat{k}_1$ are not known. Also shown in figures 1 and 2 are the local-isotropy predictions for the spectra ϕ_{θ_y} and ϕ_{θ_z} made using the measured ϕ_{θ_x} by performing the integration of $k^{-1}\phi_{\theta_x}$ in (10) for the full range of values of k_1. The measured spectra ϕ_{θ_y} and ϕ_{θ_z} decrease monotonically with increasing k as predfcted by (10) for locally isotropic turbulence. As seen from figure 1, there is excellent agreement between the measured ϕ_{θ_z} and that calculated from the isotropic relation for all dimensionless wavenumbers $k_1^* = 2\pi fy/U$ greater than about 5·0, indicating second-order local isotropy for these wavenumbers. The wavenumber $k_1^* = 5{\cdot}0$ corresponds to a wavenumber $k_1/k_d = 0{\cdot}06$, where $k_d = (\langle\epsilon\rangle/\nu^3)^{\frac{1}{4}}$ is the Kolmogorov dissipation wavenumber and ν is the kinematic viscosity. For $k_1^* < 5{\cdot}0$, the values of ϕ_{θ_z} computed from the isotropic relation lie below the measured values. The difference increases with decreasing wavenumber, consistent with the fact that $\langle(\partial\theta/\partial z)^2\rangle > \langle(\partial\theta/\partial x)^2\rangle$ for these data, while the isotropic relations employed in the theory enforce equality of the mean squares of all three components of the gradient. As shown in figure 2, the isotropic relation correctly predicts the shape of the ϕ_{θ_y} spectrum, but the absolute agreement is not as close as it is for ϕ_{θ_z}. The fact that the computed spectrum is higher than the measured one for large k_1 may be associated with the finite separation of the wires measuring $\partial\theta/\partial y$, as the data in figure 2 show that ϕ_{θ_y} is strongly attenuated with increasing Δy for this range of k_1^*. However, for smaller k_1^*, the computed curve also looks a little high, although the closer agreement for these wavenumbers as compared with that for ϕ_{θ_z} is consistent with the overall intensities measured for these data, i.e. $\langle(\partial\theta/\partial z)^2\rangle > \langle(\partial\theta/\partial y)^2\rangle > \langle(\partial\theta/\partial x)^2\rangle$. The isotropic theory correctly predicts that ϕ_{θ_x} is richer in high frequency energy and poorer in low frequency energy than ϕ_{θ_y} and ϕ_{θ_z} as observed directly from analog traces and from the spectra of Sreenivasan *et al.*

In conclusion, the good agreement between the local-isotropy theory and available measurements directly demonstrates for the first time that the fine-scale structure of turbulent scalar fields can be locally isotropic with respect to one-dimensional second-order spectra of different components of the gradient vector. In view of these results, it appears likely that scalar fluctuations in other laboratory flows and in high Reynolds number atmospheric boundary-layer turbulence and other geophysical flows will also be found to be locally isotropic with respect to the present criteria. For example, one would expect to find a large range of spectral local isotropy for temperature gradients in the heated wake flow studied by Freymuth & Uberoi (1971), for which they found near equality of $\langle(\partial\theta/\partial x)^2\rangle$, $\langle(\partial\theta/\partial y)^2\rangle$ and $\langle(\partial\theta/\partial z)^2\rangle$. Hopefully, measurements of ϕ_{θ_y} and ϕ_{θ_z} in geophysical flows with large Reynolds numbers will also be made in the future.

I wish to thank Prof. R. A. Antonia for generously making the data of Sreenivasan *et al.* (1976) available to me, and Prof. S. Corrsin and a reviewer for pointing out the similarity with spectral relations for a random isotropic sound field. The work was supported by ONR Contract N00014-76-C-0702 and by National Science Foundation Grant ENG76-13147 A01.

REFERENCES

BATCHELOR, G. K. 1953 *The Theory of Homogeneous Turbulence*. Cambridge University Press.

FREYMUTH, P. & UBEROI, M. S. 1971 Structure of temperature fluctuations in the turbulent wake behind a heated cylinder. *Phys. Fluids* **14**, 2574–2580.

HELLAND, K. N. 1974 Energy transfer in high Reynolds number turbulence. Ph.D. thesis, University of California, San Diego.

HINZE, J. O. 1975 *Turbulence*, 2nd edn. McGraw-Hill.

KOLMOGOROV, A. N. 1941*a* The local structure of turbulence in incompressible viscous fluid for very large Reynolds numbers. *C.R. Acad. Sci. USSR* **30**, 301–305.

KOLMOGOROV, A. N. 1941*b* Dissipation of energy in locally isotropic turbulence. *C.R. Acad. Sci. USSR* **32**, 16–18.

PANCHEV, S. 1971 *Random Functions and Turbulence*. Pergamon.

SREENIVASAN, K. R., DANH, H. Q. & ANTONIA, R. A. 1976 Temperature dissipation fluctuations in a turbulent boundary layer. *Proc. IUTAM Symp. Structure of Turbulence and Drag Reduction. Phys. Fluids Suppl.* (in press).

VAN ATTA, C. W. & CHEN, W. Y. 1969 Measurements of spectral energy transfer in grid turbulence. *J. Fluid Mech.* **38**, 743–764.